Peña-Rojas, LE.; Barrios Peña, MI.; Francés, F. (2016). Flood quantiles scaling with upper soil hydraulic properties for different
land uses at catchment scale. Journal of Hydrology. 541:1258-1272.
doi:10.1016/j.jhydrol.2016.08.031

Flood quantiles scaling with upper soil hydraulic properties for different land uses at catchment scale

Luis E. Peña[abc], Miguel Barrios[b], Félix Francés[c]

[a] Civil Engineering Program, Engineering Faculty, Universidad de Ibagué, Carrera 22 calle 67 B/Ambalá, 730001, Ibagué, Colombia

[b] Faculty of Forest Engineering, Universidad del Tolima, B/Santa Helena, 730006299, Ibagué, Colombia

[c] Research Institute on Water and Environmental Engineering, Universitat Politècnica de València, Camino de Vera s/n, 46022 Valencia, Spain

Abstract

Changes in land use within a catchment are among the causes of non-stationarity in the flood regime, as they modify the upper soil physical structure and its runoff production capacity. This paper analyzes the relation between the variation of the upper soil hydraulic properties due to changes in land use and its effect on the magnitude of peak flows: 1) incorporating fractal scaling properties to relate the effect of the static storage capacity (the sum of capillary water storage capacity in the root zone, canopy interception and surface puddles) and the upper soil vertical saturated hydraulic conductivity on the flood regime; 2) describing the effect of the spatial organization of the upper soil hydraulic properties at catchment scale; 3) examining the scale properties in the parameters of the Generalized Extreme Value (GEV) probability distribution function, in relation to the upper soil hydraulic properties. This study considered the historical changes of land use in the Combeima River catchment in South America, between 1991 and 2007, using distributed hydrological modeling of daily discharges to describe the hydrological response. Through simulation of land cover scenarios, it was demonstrated that it is possible to quantify the magnitude of peak flows in scenarios of land cover changes through its Wide-Sense Simple Scaling with the upper soil hydraulic properties.

Keywords: Land use change, scaling, hydraulic properties of soil, flood regime, GEV distribution

1. Introduction

Historically, changes in land use have taken place due to human activities as agriculture, forestry, settlements, and roadway construction (Bronstert, 2003). These activities interact to create combined effects on the flow regimes, altering significantly flood frequency distribution (Whitfield, 2012). Hence, the evaluation of changes in land use and their effect on the hydrological response at catchment scale is one of the fundamental challenges in Hydrology (Elfert & Bormann, 2010). Studies on this topic have demonstrated changes in the hydrologic regime because of land cover changes, although this effect is difficult to quantify (Alaoui *et al*., 2014), especially in the long term and at catchment scale for flood regime, because their intensity is a function of the size of the change (in relation to total area), slope, type of soil and characteristics of the precipitations (Quilbé *et al*., 2008).

Transitions from grasslands to forests and crops could represent a potential to reduce flood risk, given their contribution to diminish maximum flows, especially at small catchments as reported by Marshall et al, (2014). And vice versa, the transition from forest to grassland increases the rate and total runoff during storms (Mao & Cherkauer, 2009).

Likewise, land use changes and climatic variability induce short-term changes in peak flows (Jung et al., 2011). Additionally, it has been accepted that increased runoff is associated to increased imperviousness in the catchments, which contributes to increased flood peaks, due to the decrease of surface infiltration and deep percolation (Wijesekara et al., 2012). Mao and Cherkauer (2009) found increased runoff and reduction in evapotranspiration for the conversion of forests to grasslands, and a rise in evapotranspiration and a decline in runoff rates for the transition from grassland to crops. Similar behavior has been observed in pasture areas that were later changed to shrubs, which modified the characteristics of hillside soils, increasing runoff and reducing infiltration (Abrahams *et al*., 1995). Diminished runoff and attenuated response to flood events triggered by rainfall have been observed in reforestation scenarios

(Eckhardt et al., 2003). Such effects of land use changes on runoff are mainly attribuable to gradual alterations of soil hydraulic properties as infiltration capacity and saturated hydraulic conductivity (Gupta *et al*., 2006; Zhou *et al*., 2008).

Changes in land use modify the texture and chemical characteristics of soil (Koinig *et al*., 2003), and–in turn–its saturated hydraulic conductivity. Saturated hydraulic conductivity is a function of the size and continuity of the structure of pores in the soil and it changes gradually over time (Kumar *et al*., 2008). Changes in saturated hydraulic conductivity could also be induced by man-made actions, like tillage and irrigation of crops (Bhattacharyya *et al*., 2006). This is related to the type of vegetation and depth of its roots, which influence the soil hydraulic behavior . Hence, changes in land use induce changes in the soil infiltration capacity, which determines the hydrological response of the catchments (Zhang *et al*., 2001) and alters the flow variability pattern (Hopmans *et al*., 2002).

Based on field measurements, Kumar *et al*. (2008) found hydraulic conductivity increased in transition from grassland to agroforestry buffers. It has been as well shown that hydraulic conductivity was reestablished upon performing measurements on lands dedicated to grasslands, which then evolved to crops, indicating that the variation is due to the modification of pore distribution in the soil structure (Kodesová *et al*., 2011). In lands with transition from grasslands to forests, diminished soil erosion was observed, along with increased water availability in plants and reduced flood risk (Agnese *et al*., 2011). It is widely believed that the mean volume of pores is higher for forest soils and lower for crops and grasslands, thereby influencing the soil hydraulic conductivity values (Chen *et al*., 2009).

It has been accepted that water storage in the soil is controlled by the geometry of pore spaces and the soil structure (Schwärzel *et al*., 2011), which determine the soil humidity retention capacity and infiltration. These in turn are influenced by soil composition, type of vegetation, and depth of the roots (Hu *et al*., 2009). In forest soils, greater water content and high hydraulic

79 conductivity have been found in the root zone (Niemeyer *et al*., 2014), whereas the opposite
80 occurs for soils with grassland (Zimmermann *et al*, 2006). Thus, water storage processes in the
81 root zone , surface flow, infiltration, and water retention in the landscape are mainly relevant in
82 runoff generation during storms (Salazar *et al*., 2012) and are essential in the distribution of
83 flood frequency and magnitude (De Michele & Salvadori, 2002).

84 Evaluation of the hydrological response of catchments under scenarios of land use changes has
85 been based on the analysis of exceedance probabilities in flow series (Burn & Whitfield, 2015;
86 McCormick *et al*., 2009), the identification of runoff characteristics through hydraulic simulation,
87 analysis of satellite images, and use of geographic information systems (Sajikumar & Remya,
88 2014). Numerical simulation and generation of synthetic rainfall have also been used to
89 determine the effect of land use changes (Kuraś *et al*., 2012). Hydrological modeling has
90 permitted considering evapotranspiration variation, surface flow, and infiltration capacity,
91 which is determined by root depth (Öztürk *et al*., 2013) and modifies the soil hydraulic properties
92 according to land use changes (Salemi *et al*., 2013). Several hydrological models have been used
93 to compare these effects (see for example Cornelissen *et al*., 2013).

94 Understanding the impact of land use change on the hydrology at catchment scale may facilitate
95 to design strategies for sustainable development of water resources (Ghaffari *et al*., 2010). Our
96 assumption is that land use changes modify soil hydraulic characteristics. The main aim of this
97 paper is then to describe and analyze the effect of changes of upper soil hydraulic properties on
98 the flood regime based on hydrological modeling, and exploring the potential scaling of
99 maximum annual flows with these soil properties.

100

2. Materials and Methods

2.1. Study area

The Combeima River catchment (Fig. 1) is located in the mountainous zone of the Colombian Andes. The closing point was defined at the 2121180-Montezuma hydrometric station, which is located at an elevation of 1450 m and covers an area of 217.29 Km^2. This study used daily information reported by this hydrometric station and nine weather stations (Fig. 2) during the period between 1971 and 2012 (García *et al*., 2016).

Precipitation in the lower Combeima River catchment is higher than in its upper basin (Fig. 2), it presents a bimodal annual distribution and it has a mean of 1673 mm/year. The annual mean flow is 5.6 m^3s^{-1}. Rainfall datasets are scarce in the catchment for the altitude range of 2200 to 5150 m.a.s.l. For improving the spatial representation of rainfall, three virtual rainfall stations were generated using a Pearson's correlation weighting approach with two rainfall stations located near to Combeima catchment at 3280 and 4150 m.a.s.l. However this catchment was selected because of information availability on land use historical evolution, so its effect on the hydrological response of mountainous catchments in tropical latitudes can be analyzed.

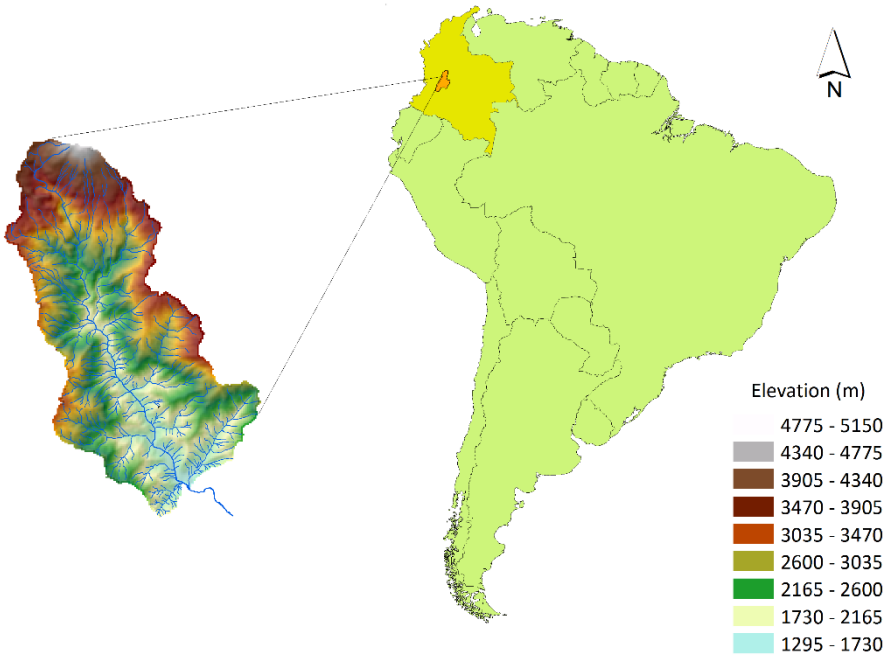

116

117 **Fig. 1**. Descriptive map of the Combeima River catchment

118

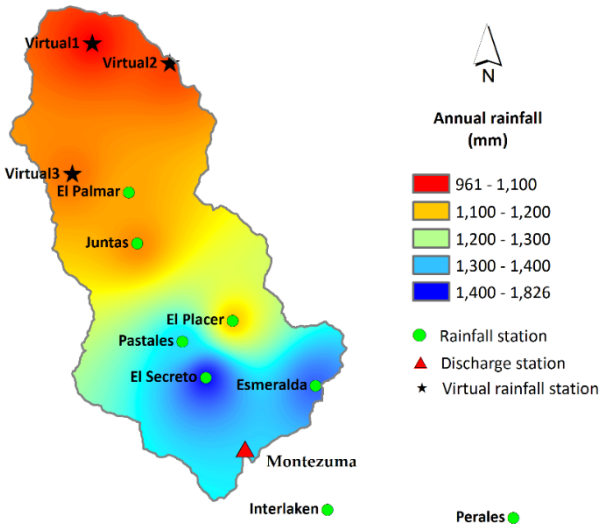

119

120 **Fig. 2.** Combeima River catchment spatial variation of annual rainfall for the period 1971-2012.

121

122 The main types of land cover in the Combeima River catchment are forest, grasslands, crops and
123 impervious areas. The forests are composed mainly by tropical evergreen forest (ARALIACEAE,
124 BORAGINACEAE, COMPOSITAE, EUPHORBIACEAE, MELASTOMATACEAE, MELIACEAE, and
125 SOLANACEAE), the grasslands are dedicated to livestock and the main crops in the region are

126 coffee, lulo fruit, blackberry and corn (*Coffea sp, Solanum quitoense, Morus sp* and *Zea mays*,
127 respectively). The impervious areas represent a relative low percentage of the catchment and
128 are related to small villages, rock outcrops and glaciers. However, the spatial distribution of land
129 cover has changed in time. In 1991, 48.9% of the Combeima River catchment was comprised of
130 forests, 20.3% crops, 28.3% grasslands and 2.5% impervious surfaces. Later, in 2000, land use
131 changes resulted in decreased forest (45.9%) and crop areas (13.8%), and increased grassland
132 areas (38.9%). This trend was reversed in 2002, when crop (17.8%) and forest areas (46.1%)
133 increased while grassland areas decreased (33.1%). Finally, in 2007, trends in land use changes
134 forest (49.1%) and crop areas (21.5%) increased and grassland areas (27%) decreased, as a result
135 of implementing environmental regulations in the region.

136 To describe land use changes, maps of soil types and land use were integrated resulting data of
137 sand, silt, clay and organic matter contents, as well as root depth for each land use, which were
138 used to generate maps of the hydraulic properties of soil, employing the pedotransfer function
139 presented by Saxton and Rawls (2006). The variations of the interception capacity and
140 evapotranspiration were incorporated depending on the types of land use considered in this
141 study (Table 1).

142 According to the study conducted by the Colombian Geographic Institute (IGAC), soils in the
143 upper basin are deep clay-loams of volcanic origin, well drained, with medium to coarse
144 textures, slopes greater than 50%, and high content of organic matter (MDA, MGC and MKG
145 units). Bedrock outcrops (MAA units) are observed in the highest elevation of the catchment,
146 corresponding to the volcanic cone. Soils in the middle basin are clay-sands from the MGB unit,
147 with low depth and high content of organic matter. Soils in the MKB unit are clay-loams and
148 clay-sands with slopes greater than 50%, rich in organic matter and well drained. The soils in
149 MQO unit coincide with the main stem of the basin, have slopes between 3% and 7%, are prone
150 to flooding and are basically alluvial sediment soils, with medium to coarse textures and low

content of organic matter. The MQC units are located in slope areas between 50% and 70%, are deep, with medium to moderately fine textures and are rich in organic matter. Soils in the MQD unit in the low basin are clay-loams and clay-gravels with slopes between 20% and 50%, low depths and highly drained. Finally, NP unit corresponds to the glacial zone (Fig.3).

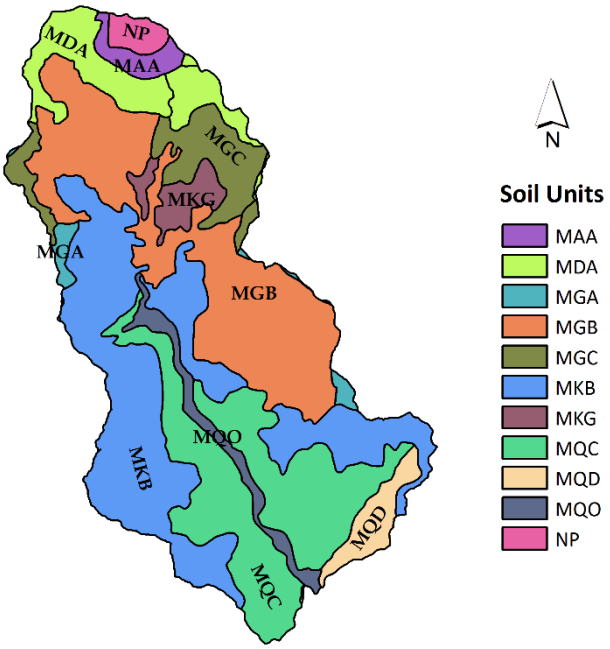

Fig. 3. Soil units in the Combeima River catchment (legend explanation in the text).

2.2. Hydrologic modeling

The hydrological model used in this paper was TETIS. It is a conceptual distributed hydrological model, with physically sound parameters, able to perform continuous and event based simulations of the water cycle and which has been applied successfully in catchment areas ranging from less than 1 Km^2 to 60,000 Km^2, with grid cell resolutions from 30x30 m to 500x500 m and in a wide range of climates. Some examples of its successful application can be found in Francés *et al*. (2007), Vélez *et al*., (2009), Andrés-Doménech *et al*. (2010), Salazar *et al*. (2012), Bussi *et al*. (2014) and Ruiz-Villanueva *et al*. (2015).

166 According to Francés *et al*. (2007), in TETIS each cell of the spatial grid simulates the water cycle
167 through five linked compartments. Each compartment represents different hydrological
168 processes described by linear reservoirs (Fig. 4). TETIS includes modules for snowmelt, canopy
169 interception, soil capillary storage and interflow, evapotranspiration, aquifer storage and base
170 flow (connected aquifer flow). Each cell receives the flow from the upstream cell above and
171 drains to the downstream cell, following the digital elevation model flow directions.
172 Compartment or tank T0 represents the snowpack and T1 is the static storage, which represents
173 upper soil humidity below field capacity, canopy interception and storage in surface depressions
174 (puddles), the tank T2 represents water over the surface that can flow as overland runoff or
175 infiltrate, T3 is the storage in the upper part of the soil above field capacity and T4 is the water
176 storage in the aquifer. For the configuration used in this paper (the simplest), the only output
177 from T1 corresponds to evapotranspiration and overland flow, interflow and base flow drain
178 directly in the river channel network, represented by the compartment T5. Finally TETIS
179 describes the flow routing in the stream network using the Geomorphologic Kinematic Wave
180 methodology (Francés *et al*., 2007).

181

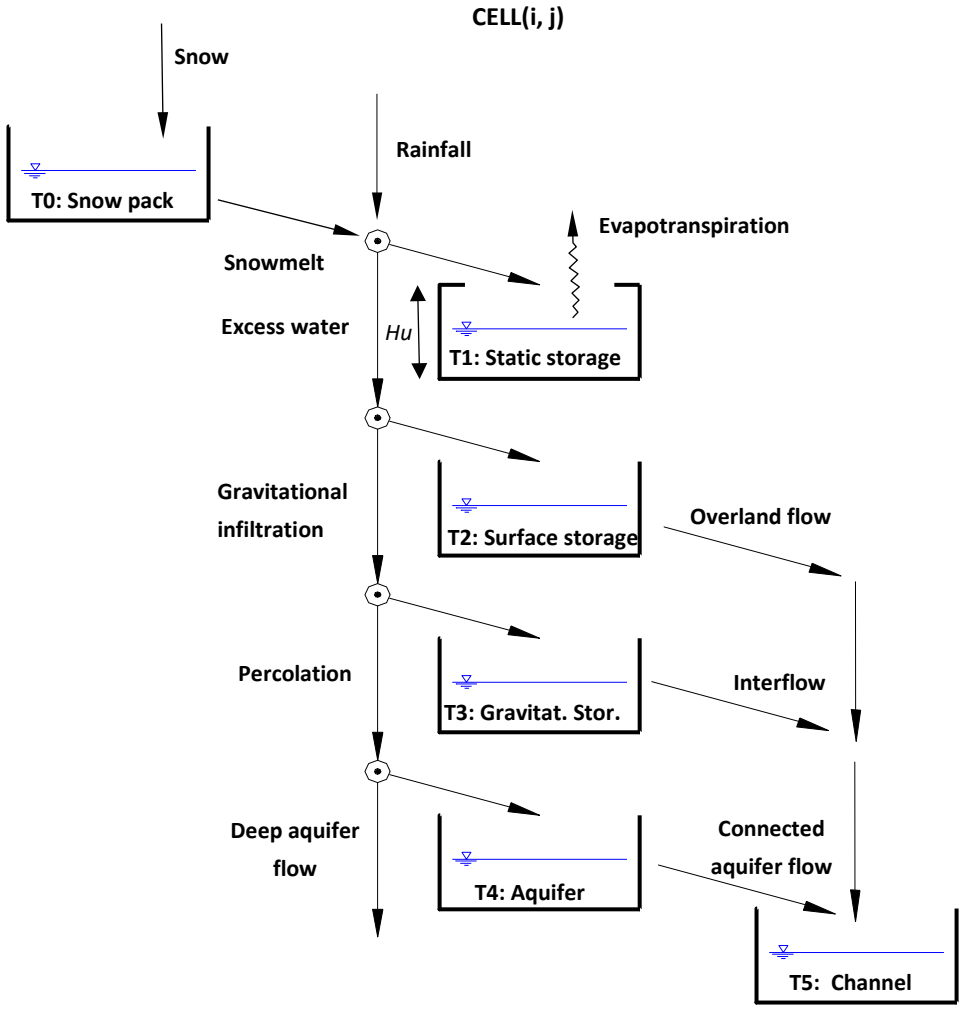

Fig. 4. Conceptual scheme of TETIS hydrological distributed model used in this paper (simplest configuration)

In this paperis focus in two parameters of the upper soil and fundamental in the runoff production: *Hu* (static storage capacity) and *Ks* (upper soil vertical saturated hydraulic conductivity). Parameter *Hu* is the storage capacity of the static tank T1 and can be estimated as:

$$H_u = \sum_i h_i AW_i + I_{max} + A_s \quad (1)$$

where h_i (mm) and AW_i are the depth and available water (the difference between the field capacity and wilting point) for each soil horizon respectively, A_s is the surface maximum depression storage (mm), which is essentially a function of land cover and topographic slope,

193 and *Imax* is the canopy maximum interception (mm). The summation in Eq. (1) is up to the
194 minimum value between soil depth and effective root depth is reached.

195 In the simplest TETIS configuration, it is assumed that the infiltration capacity is infinite below
196 field capacity, i.e., rainfall plus snowmelt go directly to T1 up to this tank is filled. Then, after T1
197 ponding, excess water con flow as overland flow through T2 or infiltrate to T3, with an infiltration
198 capacity approximately equal to the vertical saturated hydraulic conductivity of the upper soil
199 (*Ks*). This infiltration above field capacity can be called "gravitational infiltration".

200

201 **2.2.1. Parameter estimation**

202 The TETIS model parameters (including *Hu* and *Ks*) were estimated as a result of the integration
203 of various input maps: the digital elevation model, soil types, land uses, geology and geological
204 faults. The digital elevation model (DEM) of the catchment, with a grid cell size of 90x90 m, was
205 obtained from NASA's Shuttle Radar Topography Mission. The IGAC-generated maps of soil units
206 and geology and geological faults at scales of 1:500,000 and 1:25,000, respectively, were also
207 used. Maps of slopes, flow direction and overland hillside flow velocity, drainage network, and
208 cumulative cells were generated from the DEM. Percolation rate and aquifer permeability maps
209 were estimated from the geology and geological fault maps. Soil and soil substrate parameters
210 were determined by using sites sampled in each map unit (Fig. 3), corresponding to an edaphic
211 type, as reported by IGAC.

212 Land cover and land use changes were obtained based on information contained in maps for
213 1991, 2000, 2002, and 2007 of Combeima River catchment. These maps were generated by IGAC
214 at a scale of 1:25,000. Four general types of land cover and effective root depth were defined as
215 follows: forests (2.0 m), crops (0.6 m), grasslands (0.4 m) and impervious surfaces (0.0 m). Values
216 of root depth were based in Rivera (2008) and can be seen in Table 1.

217 Seasonal variation of evapotranspiration was introduced by adopting mean values of the
218 coefficient of consumptive use (λm) for each type of land cover in the catchment, based on
219 values reported by Allen *et al*. (1998) and our experience (Table 1).

220

221 The overlaying of soil type and land use maps resulted in polygons where the hydraulic
222 properties of upper soil can be estimated by using pedotransfer functions (Saxton & Rawls,
223 2006). Additionally, Eq. (1) is required for the final computation of *Hu*. The estimated parameters
224 are actually modal values (i.e., representative of the estimated characteristic rather than an
225 exact mean) and are presented in Fig. 5 for all combinations of land uses and soil types. These
226 values are assigned to each cell and, therefore, allowing the introduction of the spatial variability
227 of land use changes to each simulated scenario. The aggregations in box-plots of *Hu* and *Ks*
228 values for each land cover are displayed in Fig. 5c and 5d respectively. For this case study, there
229 is a clear *Hu* and *Ks* parameters change between the main land covers, resulting the forest land
230 cover with higher values than grassland areas.

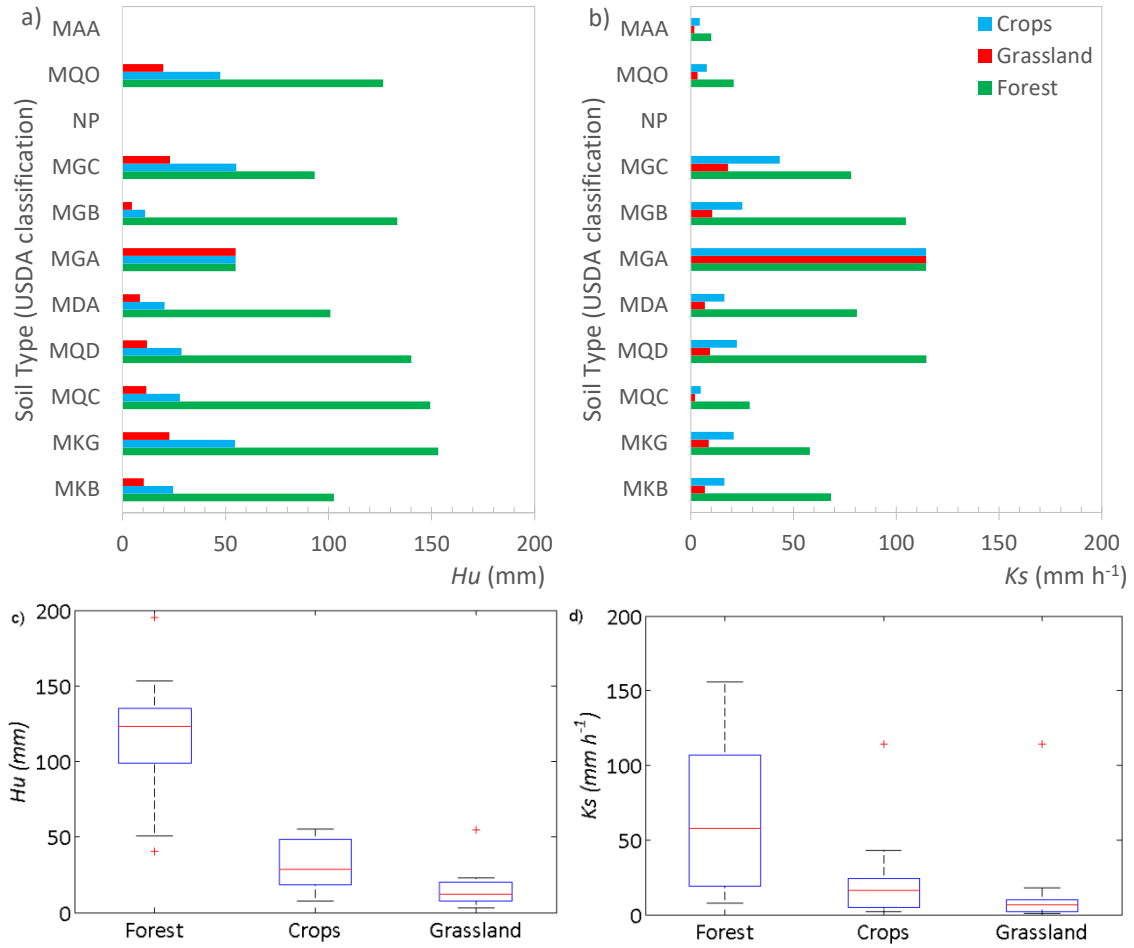

Fig. 5. Estimated upper soil hydraulic parameters by soil type and land use: a) for static storage capacity *Hu*; b) for vertical saturated hydraulic conductivity *Ks*; c and d) box-plots (aggregated by land covers) for *Hu* and *Ks* respectively.

Table 1. Consumptive use λ_m and interception capacity I_{max} used in the implementation of the hydrological model

Land cover	λ_{jan}	λ_{feb}	λ_{mar}	λ_{apr}	λ_{may}	λ_{jun}	λ_{jul}	λ_{ago}	λ_{sep}	λ_{oct}	λ_{nov}	λ_{dec}	I_{max} (mm)	Effective root depth (m)
Forest	0.60	0.75	0.85	1.00	1.00	1.00	1.00	1.00	1.00	0.85	0.75	0.60	9.00	2.00
Crops	0.30	0.35	0.50	0.60	0.77	0.90	0.98	1.00	1.00	0.98	0.90	0.78	2.00	0.60
Grassland	0.48	0.60	0.75	0.85	0.87	0.90	0.90	0.87	0.85	0.80	0.65	0.60	1.00	0.40
Impervious surfaces	1.00	1.00	1.00	1.00	1.00	1.00	1.00	1.00	1.00	1.00	1.00	1.00	0.00	0.00

2.2.2. Model implementation

Effective parameters in TETIS hydrological model have a split-parameter structure (Francés et al., 2007). In this approach, parameter maps were estimated from cartographic information (soils, land cover, topography and geology, among others) and model effective parameter values were modified by a single correction factor for each parameter map. The correction factors are

242 the variables which actually are calibrated in TETIS. According to the split-parameter structure,
243 parameter maps influenced by land cover can be updated to show land cover changes, but the
244 calibrated correction factor for each parameter map is preserved. In other words, the calibrated
245 correction factors can extend the calibration to periods with different land uses and climate.

246 To calibrate the correction factors, TETIS program can performs its automatic optimization
247 through the SCE-UA method (Duan *et al*., 1994), in this paper was used the well-known Nash-
248 Sutcliffe efficiency index (NSE) as the objective function. In this case study, the calibration was
249 carried out for the 2007-2008 period, which is closest to the year with the most-recent map of
250 land uses in the Combeima River catchment and complete hydro-climatic information were
251 available, *i.e*., year 2007. Validation was carried out for the periods 1998-2000 and 1984, by
252 keeping constant the values of correction factors obtained during model calibration.

253

254 **2.2.3. Land use simulation scenarios**

255 The analysis of the effect of land use changes on the flood regime of the Combeima River
256 catchment was based on the modeling of hydrological processes through the variation of model
257 parameters associated to evapotranspiration and runoff production.

258 In addition to the reported historical land use changes, watershed planning was simulated by
259 considering the plan defined by the local environmental authority; this scenario was
260 denominated Esc1. Also, three homogeneous scenarios were included with catchment coverage
261 totally of forest, crops and grassland, in order to describe the extreme effect of each land cover
262 on the flood regime. Table 2 summarizes the land use scenarios used in this paper. All land use
263 scenarios were simulated applying the historical meteorological information for the period from
264 1971 to 2012, without correcting the possible trends in temperature and precipitation.

265

Table 2. Land use simulation scenarios.

Description	Scenario code
1991 land cover map	1991
2000 land cover map	2000
2002 land cover map	2002
2007 land cover map	2007
Land Use Plan	Esc1
Forest land cover	Forest
Crops land cover	Crops
Grassland land cover	Grassland

2.3. Statistical scaling of floods

Simple Scaling and Multi-scaling have been used during the last 20 years to study the frequency relations of spatial or regional floods and the physical mechanisms that generate them (Robinson & Sivanapalan, 1997). The application of scaling properties has been useful in predicting flows in catchments where scarce or no information is available (GREHYS, 1996; Srinivas *et al*., 2008). This is mainly because the scale exponents of flood quantiles introduce invariance with respect to the spatial flood variability. The key point in scaling analysis is to find the appropriate scale definition.

Gupta and Waymire (1990) defined Strict-Sense Simple Scaling to describe the equality of the probability distribution of precipitations (in general, any random variable *Y*) in two different scales as:

$$Y_\lambda \overset{\text{def}}{=} \lambda^\alpha Y_S \tag{2}$$

where the $\overset{\text{def}}{=}$ symbol indicates equality in the distribution of probabilities, λ is the scale factor (λ>0) and α is the scale exponent. If Y_λ have finite ordinary moments $E[Y_{\lambda t}^r]$ of *r* order and the random variables Y_λ^r and $(\lambda^\alpha Y_S)^r$ follow the same probability distribution, then the ordinary moments can be scaled in this way:

$$m_r = E[Y_\lambda^r] = \lambda^{\alpha r} E[Y_1^r] \tag{3}$$

where it must be underlined the scale exponent is a linear function of *r*. The property defined by Eq. (3) is known as Wide-Sense Simple Scaling (WSSS). According to Vaskôva (2001), WSSS may be reflected in two forms: i) identifying the linearity of the logarithm of moments *m* of order *r* expressed as $logm_r(\lambda)$ versus $log\lambda$ for each *r*; and ii) through the linearity of the scale exponent with *r*.

The GEV was selected as the probability function for flood quantile estimation in the Combeima River catchment, because it has been widely used for the analysis of extreme values, it is a generalization of the Extreme Value family (i.e., Gumbel, Weibull and LogGumbel distributions) and, more important in this paper, it has been proven to be adequate for modeling flood scaling (Villarini, 2010). The expression of its cumulative distribution function is:

$$F(Y) = exp\left\{-\left[1-\frac{\kappa(Y-\beta)}{\alpha}\right]^{\frac{1}{\kappa}}\right\} \quad (4)$$

where α, β and κ are the scale, location and shape parameter respectively. The parameters of the GEV distribution were estimated through the Maximum Likelihood (ML) method, because of its advantagesin the type of problem to be solved (see for example Morrison & Smith, 2002 and Botero & Francés, 2010). Details for the parameter estimation using ML method are given in Appendix A.

The main hypothesis in this paper is that moments and GEV parameters can be expressed as a function of the spatial average of *Hu* and *Ks*. I.e., floods follow WSSS and the GEV parameters can be given by:

$$\alpha_\lambda = \alpha_0\lambda^{-a} \quad (5)$$

$$\beta_\lambda = \beta_0\lambda^{-b} \quad (6)$$

$$\kappa_\lambda = \kappa_0\lambda^{-c} \quad (7)$$

where scale λ can be *Hu* or *Ks.*

3. Results and Discussion

3.1. Modeling of land use changes

Land uses in the Combeima River catchment were reclassified into four groups: forests, crops, grassland, and impervious surfaces; *Hu* and *Ks* values were obtained from the pedotransfer functions, as indicated in Section 2.2.1. Therefore, changes in land use changed the values of the upper soil hydraulic parameters. The resulting maps for historical land uses and planned scenarios are shown in Fig. 7. From this figure, it is clear the significant changes in the spatial distribution of upper soil hydraulic parameters between different land use scenarios.

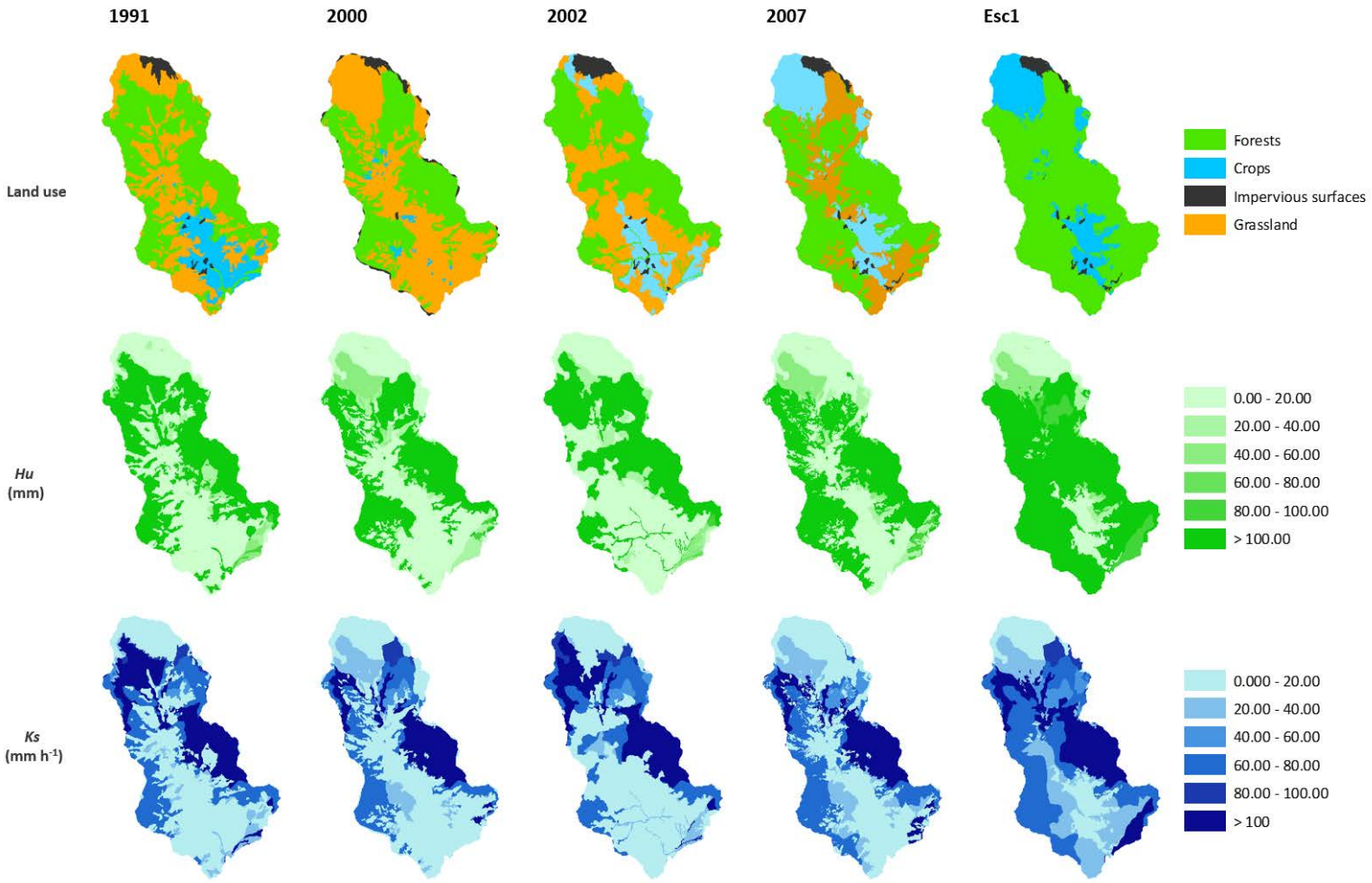

Fig. 6. Historical (period 1991-2007) and planned (Esc1) **l**and uses and values for Hu and Ks for the Combeima River catchment

For the model performance evaluation, we have used the well-known in hydrological modelling Nash-Sutcliffe efficiency index (NSE) and the Root Mean Square Error (RMSE). In calibration, a NSE value of 0.5167 and RMSE of 1.209 were obtained (2007-2008 period Fig. 8a), while in validation the NSE was equal to 0.5250 and RMSE equal to 0.981 for the period 1998-2000 (Fig.8b) and 0.5115 and 1.032 respectively for the year 1984 (Fig.8c). These modeling results are not extraordinary, but it must be underlined that the objective in this research is the scaling with land use changes, with no particular emphasis on the model performance. Also, it must be taken into account the poor information concerning the precipitation in the upper part of the catchment, as described in section 2.1. However, although the regime is different in calibration and validation periods (dryer for calibration), there is not a deterioration in the model efficiency from calibration to validation. Also, existing literature considers acceptable a Nash-Sutcliffe efficiency index greater than 0.5 for validation (Moriasi *et al*., 2007), which is the case. This is a robust acceptable model implementation, ready to test our hypothesis about flood scaling with land use changes at daily time resolution.

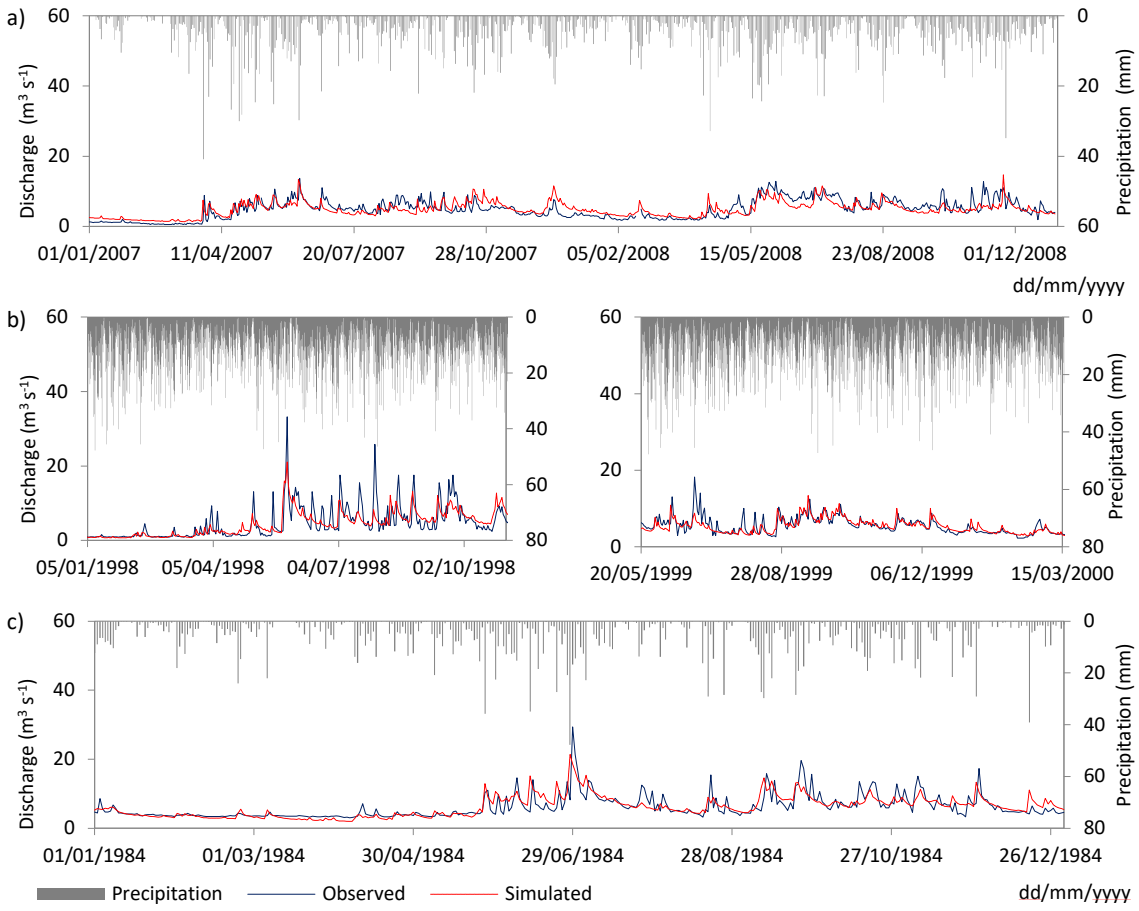

Fig. 7. Hydrologic model implementation: a) calibration period (2007-2008); b) validation period (1998-2000); c) validation period (1984).

After calibrating and validating the model, simulations of land use changes scenarios were conducted, as described in Section 2.2.3. From the results of these simulations (annual maxima for all land use scenarios can be seen in Fig. 9), it was identified that forests and crops land uses generate lower peak flows than grassland, coinciding with reports by Elfert & Bormann (2010), mainly due to the associated modal values of the upper soil hydraulic parameters *Hu* and *Ks* (see the box-plots in Fig. 5c and 5d). Grassland areas increased 37.5% while forests and crops decreased by 32.1 and 6.2% respectively between 1991 and 2000 scenarios. These changes produced an increase of 2.1% on mean annual maximum flow. In the 2007 scenario, forest and crops areas were increased by 7.0% and 55.9%, while grassland decreased in 30.5% compared to 2000 scenario. The change from 2000 to 2007 scenario produces a 7.0% decrease in the maximum annual flows. Similar

355 observations are reported by Robinson *et al*. (2003) in paired catchments. By contrast, no great
356 differences were identified in the maximum annual flows comparing 2000 and 2002 scenarios, as
357 reported by Andréassian (2004) and Geris et al. (2015).

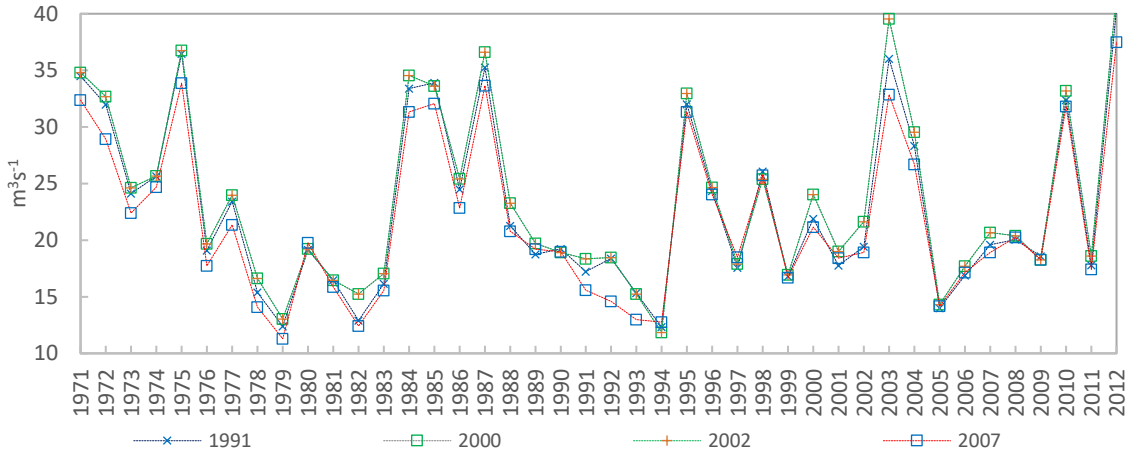

358

359 **Fig. 8.** Maximum annual flows in the Combeima River catchment for the historical land use scenarios.

360 In scenarios simulating an homogeneous land cover in the catchment (Fig. 10), it was observed more
361 significant changes. The mean maximum annual flow in forest was smaller by 12.4% than in
362 grassland scenario. Comparing forest and crops scenarios, the annual maximum flows were reduced
363 by 10.3% in average. On the other hand, for crops and grassland scenarios, an increase of 24.4% in
364 annual maximum floods was presented in the grassland scenario. Similar results have been reported
365 by Hundecha and Bárdossy (2004), Mao and Cherkauer (2009), Stehr *et al*. (2010), Udawatta *et al*.
366 (2002) and Lovell and Sullivan (2006). As can be seen in Fig. 10, the simulation of the Combeima
367 River Land Use Plan gave a similar flood regime to the forest scenario.

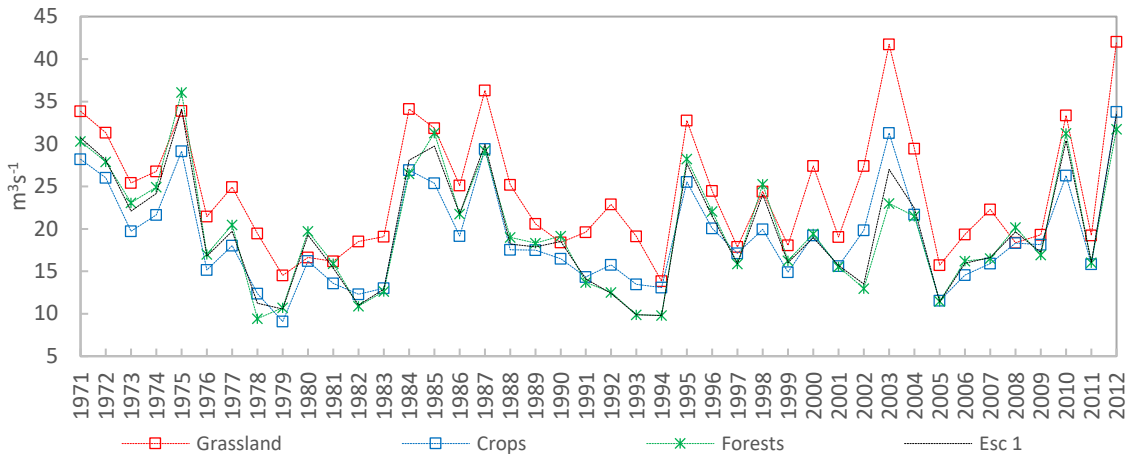

Fig. 9. Maximum annual flows in the Combeima River catchment for the homogeneous and planned (Esc1) land use scenarios.

With the hydrological simulation of homogeneous land covers, it was noted more clearly that annual flow maxima were higher for low *Hu* and *Ks* values, which are related in the Combeima River catchment to grassland cover (Figs. 5c and 5d). And the opposite: forest, with higher *Hu* and *Ks* values, produced less runoff than the crops and grasslands. Thus, the key element to explain the influence of land use changes in this case study is the estimated values of the upper soil hydraulic parameters for each land cover.

3.2. Flood scaling with *Hu* and *Ks*

Fig. 11 represents the ordinary *r* moments of the simulated annual maximum flows, m_r, as a function of the spatial mean values of *Hu* and *Ks* for the eight land use scenarios. The simulated annual maximum flows are represented in Figs. 9 and 10 and the scenarios are defined in Table 2. The homogeneous forest, crops and grassland scenarios result left to right points in Fig. 11, respectively. From this figure, it is clear the existence of a power law relationship between m_r and the spatial mean of *Hu* and *Ks*. In this case, the spatial mean values of *Hu* and *Ks* are acting as the scales (λ in Eqs. 2 and 3) and represent the main effect of different land uses in the flood regime.

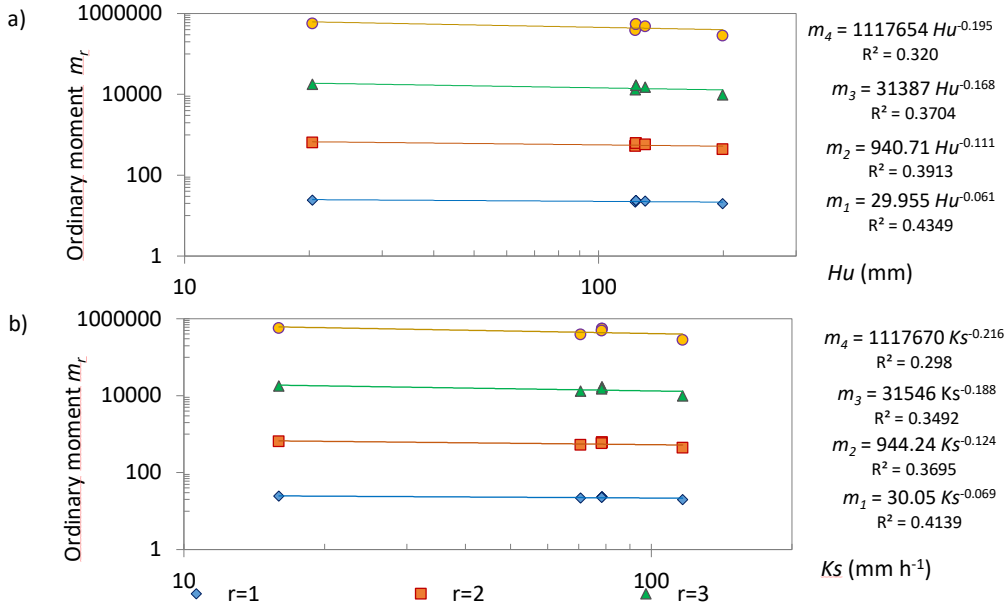

Fig. 10. Testing scaling behavior of upper soil hydraulic properties in the flood regime: a) Static storage capacity *Hu*; b) Vertical saturated hydraulic conductivity *Ks*

The slope of each fitted line in Fig. 11 is the estimated value of the scale exponent of each *r* order. Fig. 12 represents these scale exponents (different for *Hu* and *Ks*) versus the *r* order. it is clear the linear dependence defined in Eq. (3) of scale exponents with the *r* order and it proves the existence of a Wide-Sense Simple Scaling (WSSS), as defined by Gupta & Waymire (1990), for the annual maximum flows.

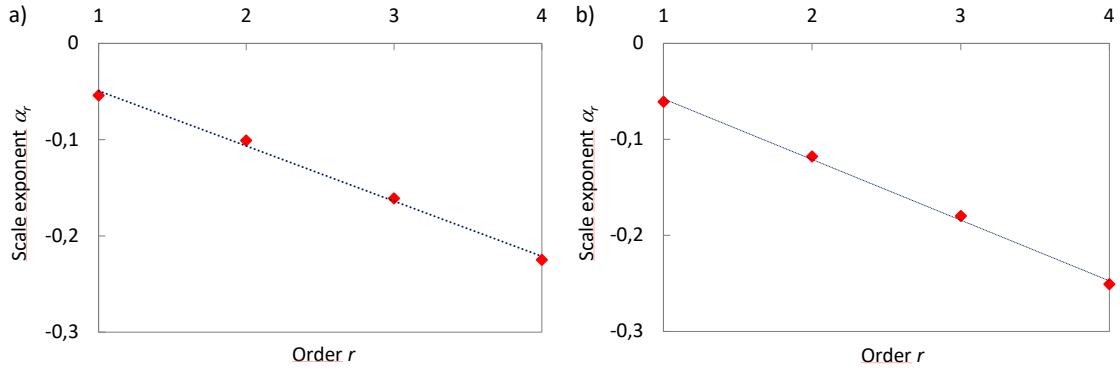

Fig. 11. Scale exponent α_r for different m_r ordinary moments as a function of *r* and linear fitting, when scale is: a) static storage *Hu*; b) vertical saturated hydraulic conductivity *Ks.*

3.3. Influence of soil heterogeneity in flood scaling

To analyze the effect of the soil spatial heterogeneity, on the hydrological response of the Combeima River catchment and the scaling property, six spatial organization patterns of *Hu* and *Ks* were proposed in the following manner:

1) Random spatial distribution (Random)

2*)* Spatial distribution according to the terrain slope (*Slope)*

3) Spatial distribution according to the Beven's Topographic Index (*IndTopo)*

and three spatial dependence based on a semivariogram that describes spherical anisotropy with the same nugget effect (300 m), sill (1500 m), range from 2500 to 15000 m, but with different semivariogram angles (0, 45 and 135°):

4) $\gamma(h)=300+1500\ \mathrm{Esf}_{15000,2500,0}$ (*A0*)

5) $\gamma(h)=300+1500\ \mathrm{Esf}_{15000,2500,135}$ (*A135*)

6) $\gamma(h)=300+1500\ \mathrm{Esf}_{15000,2500,45}$ (*A45*)

One example of these different organization patterns can be seen in Fig. 13. For each organization pattern, nine sets of statistics of *Hu* and *Ks* were considered, using three representative (for the three main land covers) mean values (μ) and three coefficient of variation (*CV*) (Table 4). A Beta probability distribution function was considered for *Hu* values (double bounded), while a Log-Normal distribution (left bounded) was used for *Ks* values (Barrios & Francés, 2012). Therefore, for this exercise, 54 *Hu* and *Ks* maps were obtained and the corresponding annual maximum flows were simulated for the complete historical record of meteorological information.

Table 3. *Ks* and *Hu* statistics used for each spatial organization pattern.

CV code	Land Use	Min *Hu*	μ *Hu*	Max *Hu*	*CV Hu*	Min *Ks*	μ *Ks*	Max *Ks*	*CV Ks*
*CV*0.1			80.31		0.101		70.595		0.101
*CV*0.3	Forest	40.4	80.20	250.0	0.326	7.9	70.600	155.6	0.326
*CV*0.5			80.54		0.502		70.610		0.501
*CV*0.1			48.76		0.102		33.646		0.100
*CV*0.3	Crops	7.9	48.76	55.2	0.326	2.0	33.627	3008.6	0.325
*CV*0.3a			48.77		0.323		33.588		0.500
*CV*0.1			20.35		0.102		15.969		0.100
*CV*0.3	Grassland	3.2	20.35	54.9	0.327	1.1	15.969	3000.6	0.326
*CV*0.3a			20.36		0.326		15.957		0.497

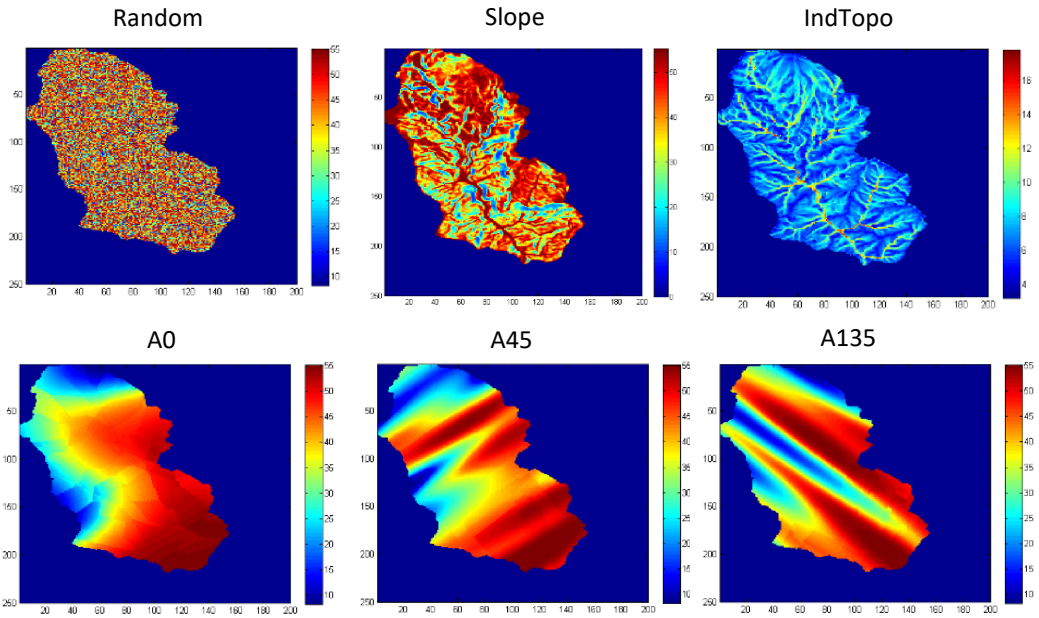

Fig. 12. *Hu* parameter maps for the six spatial organization patterns in the catchment with mean corresponding to crops and *CV* equal to 0.3 (*CV03*).

Fig. 14 displays the scale exponent for each pattern, land cover and *CV* for the parameters *Hu* and *Ks* as a function of moment orders *r*. From this figure, it can be said that there is WSSS independently of the organization pattern, but WSSS will not be possible including all of them. In fact, in Fig. 14, three groups of scaling slopes can be differentiated: 1) those following the organization patterns Slope and IndTopo with a high influence of topography, which have similar slopes for all *CV*s (from 0.1 to 0.5); 2) patterns based on spherical anisotropy (A0, A45 and A135), which have a lower slope than the previous group; and 3) the Random spatial distribution for *CV*0.1 has a similar slope to all

organization scenarios, while for *CV*0.3 its slope is similar to that of group A0 to A135 scenarios, and for *CV*0.3a its slope is located within group 1.

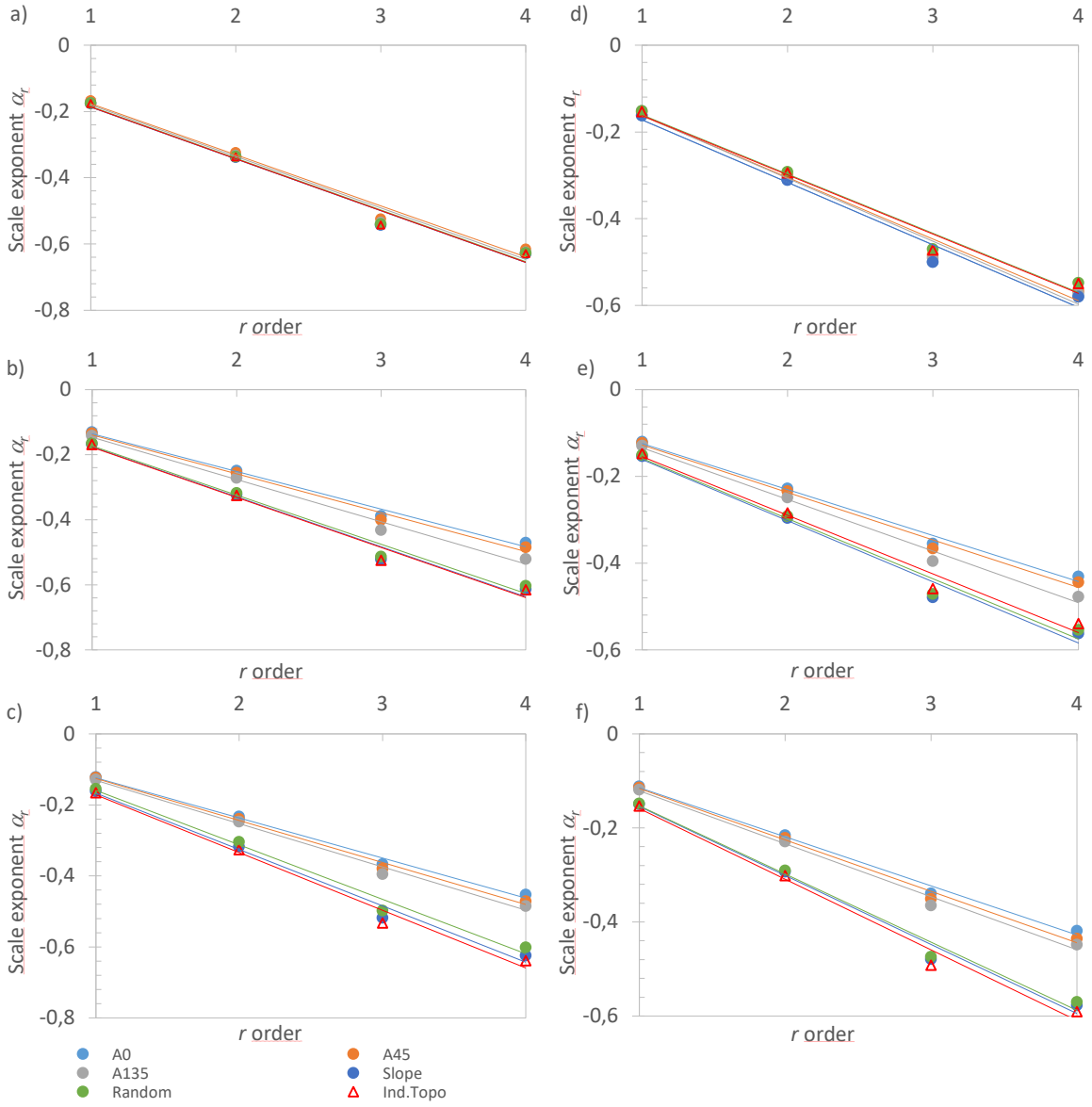

Fig. 13. Scaling exponent α_r as a function of moment order r for all spatial organization patterns and land use scenarios for: a) *Hu* with *CV*0.1; b) *Hu* with *CV*0.3; c) *Hu* witn *CV*0.5; d) *Ks* with *CV*0.1; e) *Ks* with *CV*0.3; f) *Ks* with *CV*0.3a. Lines are the fitting for each spatial organization pattern.

A high spatial uniformity in the *Hu* and *Ks* values, results in an approximately equal slope of the scale exponents in all the spatial organization patterns scenarios, indicating the strength of the scaling.

441 This occurs for scenarios with *CV* values of 0.1 (Figs. 14a and d). On the contrary, it can be observed
442 that when the spatial heterogeneity of the *Hu* and *Ks* parameters is high (Figs. 14b, c, d and f), the
443 slopes of the scaling exponent are lower, which indicates the scaling is weaker (Burlando & Rosso,
444 1996). Therefore, it may be stated that the spatial organization of the parameters does not affect
445 the existence of scaling, but it will be different and the spatial heterogeneity of the soil hydraulic
446 properties determines the strength of the WSSS.

447

448 **3.4. Scaling of the GEV distribution parameters**

449 The GEV distribution function was applied to analyze flood frequency in scenarios of land use
450 changes and test the possibility of scaling of its parameters. Table 5 and Fig. 15 resume the results
451 of this analysis. From the statistical point of view, it can be seen that all land use scenarios have
452 similar ML values, which means a similar fitting performance.

453 Concerning the impact of land use changes, it must be taken into account the uncertainty associated
454 to the estimated quantiles (only 42 years of simulated series) and, therefore, is not possible to
455 address absolute conclusions. But it can be said that in scenarios of homogeneous crops and forest
456 resulted in lower magnitudes of the maximum flows and flood quantiles compared to grasslands or
457 land use scenarios with a high percentage of pastures, as in scenarios 2000 and 2002. These results
458 are similar to those found by Kumar *et al*. (2008), Elfert & Bormann (2010), Nie *et al*. (2011) and
459 Salazar et. (2012). Also, it can be mentioned from Fig. 15 that the flood regime of land use planning
460 scenario (Esc1) is more similar to a homogeneous forest land cover, and the historical land use
461 scenarios are more similar to the grassland scenario. Different land uses can change significantly the
462 flood regime depending on the intensity of the land use change and the case study: for example,

463 the 100 years return period flood quantile in the Combeima River catchment can vary between 38

464 to 53 m^3/s (a 40% difference).

465 **Table 4**. For each land use scenario, spatial mean of the upper soil hydraulic parameters, flood sample statistics and
466 parameters and flood quantiles using the GEV.

Land use scenario	Upper soil parameters		Flood sample statistics				ML GEV parameters				Flood quantiles (m^3/s)				
											Return period (years)				
	Hu	*Ks*	μ	η	γ	k	β	α	κ	Maximum Likelihood	5	10	25	50	100
2007	122.748	70.599	21.786	0.325	0.601	2.079	-0.047	5.388	18.379	-138.506	26.754	31.174	36.988	41.473	46.075
2002	123.111	78.534	23.537	0.334	0.738	2.275	-0.109	5.644	19.67	-141.705	28.869	34.069	41.281	47.135	53.408
2000	123.111	78.534	23.537	0.334	0.738	2.275	-0.109	5.645	19.673	-141.705	28.871	34.069	41.276	47.125	53.392
1991	129.699	78.38	22.79	0.337	0.705	2.157	-0.129	5.416	18.902	-140.652	27.862	33.036	40.331	46.346	52.881
Esc1	163.436	92.121	19.758	0.348	0.482	2.068	0.05	5.672	16.681	-138.368	24.879	28.757	33.456	36.801	40.008
Forest	199.472	116.676	19.778	0.352	0.466	2.223	0.094	5.923	16.801	-139.098	25.086	28.813	33.161	36.145	38.918
Crops	48.88	33.634	19.117	0.31	0.748	2.553	-0.014	4.58	16.39	-130.75	23.33	26.855	31.361	34.742	38.129
Grassland	20.367	15.971	24.316	0.3	0.77	2.559	-0.106	5.232	20.696	-138.613	29.201	33.991	40.613	45.974	51.705

467 Sample statistics: mean μ, coefficient of variation η, skewness coefficient γ and kurtosis coefficient k.

468

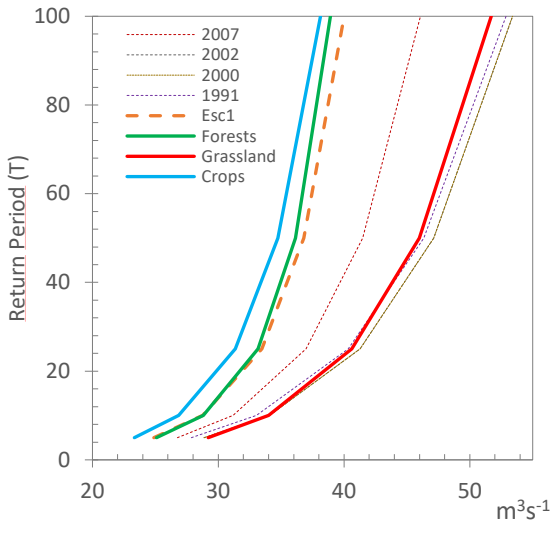

469

470 **Fig. 14**. Estimated flood quantiles using the GEV distribution for all land use scenarios.

471

472 Fig. 16 shows, that the α and κ GEV parameters follow a power law with respect to the upper soil
473 hydraulic properties, as described by Eqs. 5 and 6. The fitted equations are given in this figure. On
474 the other hand, there are negative values for the estimated β values, which is incompatible with a

power law (Figs. 16 b and e). However, the actual magnitude of floods makes the estimated β s relatively close to zero, and the equation $\beta_\lambda = 0$ is a special case of power law. A GEV with null β collapses into a Weibull distribution and, at the same time, the WSSS property is satisfied.

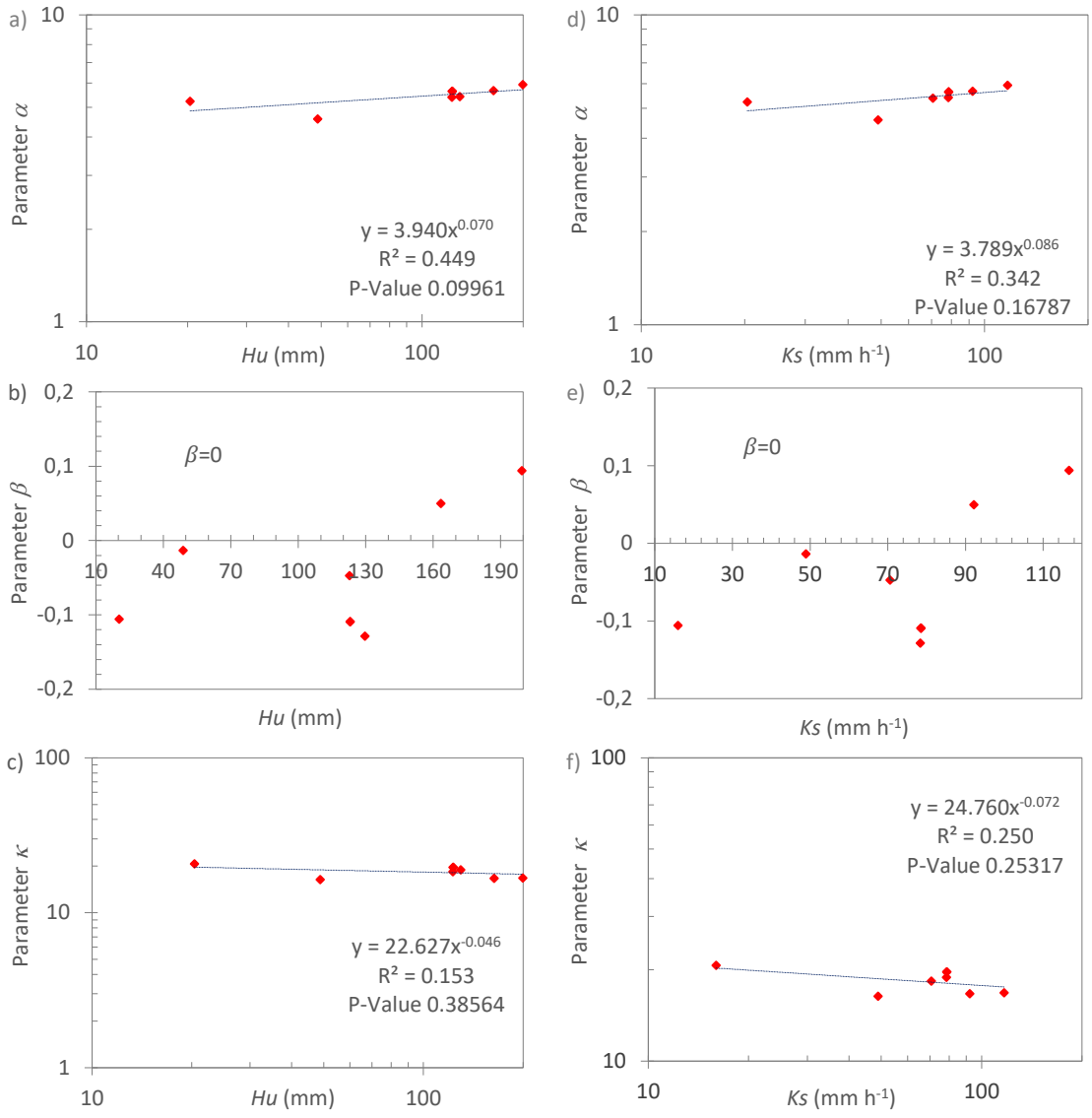

Fig. 15. Scaling behavior of GEV distribution parameters: a, b, c) scale, location and shape respectively for *Hu*; d, e, f) idem for *Ks*.

It is clear that in some cases the regressions are relatively strong (maximum R2 equal to 0.45) and in others are weak (minimum R2 equal to 0.15). In terms of p-values the equivalent are 0.1 and 0.39 respectively. In terms of critical values for correlation the critical values are 0.582 for α=0.1 and 0.754 for α=0.05. Of course these numbers are not showing a perfect scaling of the GEV parameters, but working with real Nature these regressions can be acceptable.

4. Conclusions

Land use change scenarios are reflected in the hydrological model TETIS by changes in evapotranspiration and runoff production parameters. In particular, for flood regime characterization, its upper soil hydraulic parameters *Hu* and *Ks* are the more important characteristics. Given that this study adopted modal values for *Hu* and *Ks* using pedotransfer functions, more research is needed to contrast the results presented in this paper with empirical values of the evolution and change of upper soil hydraulic properties with land use changes.

Through hydrological simulation of different land use scenarios in the Combeima River catchment for the whole historical period 1971-2012, it was found that annual maximum flows and flood quantiles can be sensible to land use changes, depending on the intensity of the land use change. In this case study, floods presented higher magnitudes for grassland cover and lower for forests and crops land uses. Or vice versa: transitions from grasslands to forests or crops could reduce floods magnitude. However, in some cases it may not have a significant effect on the magnitude of annual flow maxima, as observed in Combeima River catchment if 2000 and 2002 scenarios are compared.

For each land use scenario, sample ordinary moments were estimated from the 42 years of simulated maximum annual flows. It was clear that ordinary moments are invariant using as scale the catchment spatial mean of *Hu* and *Ks.* Actually, the scaling can be considered Wide-Sense Simple Scaling (WSSS) due to the linear relationship between the scale exponents of the ordinary *r* moments and the moment order m_r.

The effect of the spatial variability of the upper soil hydraulic properties within the catchment area was evaluated through the simulation of different spatial organization patterns. It was found that spatial pattern influences the flood behavior, but maintaining the WSSS property. In other words,

floods are fractals with the appropriated scale related with the main runoff production characteristics at catchment scale.

Scalable behavior was also found in the parameters of the fitted GEV distribution to the simulated annual maxima, in relation to the catchment spatial mean of *Hu* and *Ks* parameters. Moreover, through the determination of *Hu* and *Ks* for different land use scenarios, it is possible to obtain flood quantiles by exploiting the WSSS with a minimum of simulations. This could represent a very valuable tool for environmental planning and flood risk management at catchment scale, especially in areas with scarce or no hydrometric information.

Acknowledgements. This research was funded partially by the COLCIENCIAS 567 doctoral fellowship program, Universidad del Tolima project 1300213 and Universidad de Ibagué (Colombia) project 12-262-COL00, and by Universitat Politècnica de València (Spain) and by the Spanish Research Project ECO-TETIS (ref. CGL2011-28776-C02-01) and TETIS-MED (ref. CGL2014-58127-C3-3-R). Thanks to *The Shuttle Radar Topography Mission NASA, IDEAM* and *IGAC in* Colombia, for providing digital elevation model, streamflow, rainfall data, and soil study of the Tolima Region.

Appendix A. GEV parameter estimation by ML method

Estimation of GEV parameters through ML method is done in this research solving the next system of non-linear equations:

$$\frac{1}{\alpha}\sum_{i=1}^{N}\left[\frac{1-k-(Y_i)^{1/k}}{Y_i}\right]=0 \qquad (A.1)$$

$$-\frac{N}{\alpha}+\frac{1}{\alpha}\sum_{i=1}^{N}\left[\frac{1-k-(Y_i)^{1/k}}{Y_i}\left(\frac{Y_i-\beta}{\alpha}\right)\right]=0 \qquad (A.2)$$

$$-\frac{1}{k^2}\sum_{i=1}^{N}\left\{\ln Y_i\left[1-k-(Y_i)^{\frac{1}{k}}\right]+\frac{1-k-(Y_i)^{\frac{1}{k}}}{Y_i}k\left(\frac{Y_i-\beta}{\alpha}\right)\right\}=0 \qquad (A.3)$$

The convergence criterion for each of these equations is given respectively by:

$$\frac{\sum_{i=1}^{N} exp^{-\left[-\ln\left(1-\left(\frac{Y-\beta}{\alpha}\right)k\right)^{\frac{1}{k}}\right]+\left(k-\left(-\ln\left(1-\left(\frac{Y-\beta}{\alpha}\right)k\right)^{\frac{1}{k}}\right)\right.} - (1-k)\sum_{i=1}^{N} exp^{k-\ln\left(1-\left(\frac{Y-\beta}{\alpha}\right)k\right)^{\frac{1}{k}}}}{\hat{\alpha}} \approx 0 \quad \text{(A.4)}$$

$$\frac{1}{\alpha}\left(\frac{N-\sum_{i=1}^{N} exp^{--ln\left(1-\left(\frac{Y-\beta}{\alpha}\right)k\right)^{\frac{1}{k}}} + \sum_{i=1}^{N} exp^{-\left[-\ln\left(1-\left(\frac{Y-\beta}{\alpha}\right)k\right)^{\frac{1}{k}}\right]+\left(k-\left(-\ln\left(1-\left(\frac{Y-\beta}{\alpha}\right)k\right)^{\frac{1}{k}}\right)\right.} - (1-k)\sum_{i=1}^{N} exp^{k-ln\left(1-\left(\frac{Y-\beta}{\alpha}\right)k\right)^{\frac{1}{k}}}}{\hat{\beta}}\right) \approx 0 \quad \text{(A.5)}$$

$$\frac{1}{k}\left\{\left(N-\sum_{i=1}^{N}-\ln\left[1-\left(\frac{Y-\beta}{\alpha}\right)k\right]^{\frac{1}{k}}+\sum_{i=1}^{N}-\ln\left[1-\left(\frac{Y-\beta}{\alpha}\right)k\right]^{\frac{1}{k}} exp^{-\left[-\ln\left(1-\left(\frac{Y-\beta}{\alpha}\right)k\right)^{\frac{1}{k}}\right]}\right)\right.$$
$$\left.-\left(\frac{N-\sum_{i=1}^{N} exp^{-\left[-\ln\left(1-\left(\frac{Y-\beta}{\alpha}\right)k\right)^{\frac{1}{k}}\right]} + \sum_{i=1}^{N} exp^{-\left[-\ln\left(1-\left(\frac{Y-\beta}{\alpha}\right)k\right)^{\frac{1}{k}}\right]+\left[k-\left(-\ln\left(1-\left(\frac{Y-\beta}{\alpha}\right)k\right)^{\frac{1}{k}}\right]\right.} - (1-k)\sum_{i=1}^{N} exp^{k-\ln\left[1-\left(\frac{Y-\beta}{\alpha}\right)k\right]^{\frac{1}{k}}}}{\hat{\alpha}}\right)\right\} \approx 0 \quad \textit{(A.6)}$$

References

Abrahams, A. D., Parsons, A. J., & Wainwright, J. (1995). Effects of vegetation change on interrill runoff and erosion, Walnut Gulch, southern Arizona. *Geomorphology*, *13*(1-4), 37–48. doi:10.1016/0169-555X(95)00027-3

Agnese, C., Bagarello, V., Baiamonte, G., & Iovino, M. (2011). Comparing Physical Quality of Forest and Pasture Soils in a Sicilian Watershed. *Soil Science Society of America Journal*, *75*(5), 1958. doi:10.2136/sssaj2011.0044

Alaoui, A., Willimann, E., Jasper, K., Felder, G., Herger, F., Magnusson, J., & Weingartner, R. (2014). Modelling the effects of land use and climate changes on hydrology in the Ursern Valley, Switzerland. *Hydrological Processes*, *28*(10), 3602–3614. doi:10.1002/hyp.9895

Allen, R. G., Pereira, L. S., Raes, D., & Smith, M. (1998). *Crop evapotranspiration: Guidelines for computing crop requirements*. *Irrigation and Drainage Paper No. 56, FAO*. doi:10.1016/j.eja.2010.12.001

Andréassian, V. (2004). Waters and forests: From historical controversy to scientific debate. *Journal of Hydrology*, (291), 1–27. doi:10.1016/j.jhydrol.2003.12.015

Andrés-Doménech, I., Múnera, J. C., Francés, F., & Marco, J. B. (2010). Coupling urban event-based and catchment continuous modelling for combined sewer overflow river impact assessment. *Hydrology and Earth System Sciences*, *14*, 2057–2072. doi:10.5194/hess-14-2057-2010

Barrios, M., & Francés, F. (2012). Spatial scale effect on the upper soil effective parameters of a distributed hydrological model. *Hydrological Processes*, *26*(7), 1022–1033. doi:10.1002/hyp.8193

Bhattacharyya, R., Prakash, V., Kundu, S., & Gupta, H. S. (2006). Effect of tillage and crop rotations on pore size distribution and soil hydraulic conductivity in sandy clay loam soil of the Indian Himalayas. *Soil and Tillage Research*, *86*(2), 129–140. doi:10.1016/j.still.2005.02.018

Botero, B. A., & Francés, F. (2010). Estimation of high return period flood quantiles using additional non-systematic information with upper bounded statistical models. *Hydrology and Earth System Sciences*, *14*(12), 2617–2628. doi:10.5194/hess-14-2617-2010

Bronstert, A. (2003). Floods and climate change: interactions and impacts. *Risk Analysis : An Official Publication of the Society for Risk Analysis*, *23*(3), 545–57. Retrieved from http://www.ncbi.nlm.nih.gov/pubmed/12836847

Burlando, P., & Rosso, R. (1996). Scaling and multiscaling models of depth-duration-frequency curves for storm precipitation. *Journal of Hydrology*, *187*, 45–64. doi:10.1016/S0022-1694(96)03086-7

Burn, D. H., & Whitfield, P. H. (2015). Changes in floods and flood regimes in Canada. *Canadian Water Resources Journal / Revue Canadienne Des Ressources Hydriques*, (August 2015), 1–12. doi:10.1080/07011784.2015.1026844

566 Bussi, G., Frances, F., Montoya, J. J., & Julien, P. Y. (2014). Distributed sediment yield modelling: Importance of inicial
567 sediment conditions. *Environmental Modelling and Software*, (58), 58–70.
568 Chen, X., Zhang, Z., Chen, X., & Shi, P. (2009). The impact of land use and land cover changes on soil moisture and hydraulic
569 conductivity along the karst hillslopes of southwest China. *Environmental Earth Sciences*, *59*(4), 811–820.
570 doi:10.1007/s12665-009-0077-6
571 Cornelissen, T., Diekkrüger, B., & Giertz, S. (2013). A comparison of hydrological models for assessing the impact of land
572 use and climate change on discharge in a tropical catchment. *Journal of Hydrology*, *498*, 221–236.
573 doi:10.1016/j.jhydrol.2013.06.016
574 De Michele, C., & Salvadori, G. (2002). On the derived flood frequency distribution : analytical formulation and the in
575 fluence of antecedent soil moisture condition. *Journal of Hydrology*, *262*, 245–258. doi:10.1016/S0022-
576 1694(02)00025-2
577 Duan, Q., Sorooshian, S., & Gupta, V. (1994). Optimal use of the SCE-UA global optimization method for calibrating
578 watershed models. *Journal of Hydrology*, *158*(3-4), 265–284. doi:10.1016/0022-1694(94)90057-4
579 Eckhardt, K., Breuer, L., & Frede, H. (2003). Parameter uncertainty and the significance of simulated land use change
580 effects. *Journal of Hydrology*, *273*(1-4), 164–176. doi:10.1016/s0022-1694(02)00395-5
581 Elfert, S., & Bormann, H. (2010). Simulated impact of past and possible future land use changes on the hydrological
582 response of the Northern German lowland "Hunte" catchment. *Journal of Hydrology*, *383*(3-4), 245–255.
583 doi:10.1016/j.jhydrol.2009.12.040
584 Francés, F., Vélez, J. I., & Vélez, J. J. (2007). Split-parameter structure for the automatic calibration of distributed
585 hydrological models. *Journal of Hydrology*, *332*(1-2), 226–240. doi:10.1016/j.jhydrol.2006.06.032
586 García, B., Peña, L. E., Barrios, M., & Múnera, J. (2016). Uncertainty of discharge estimation in high-grade Andean streams.
587 *Flow Measurement and Instrumentation*, *48*, 42–50. doi:10.1016/j.flowmeasinst.2016.02.005
588 Geris, J., O'Connell, E., Greg, O., & Will, M. (2015). *Multiscale experimentation , monitoring and analysis of long-term land*
589 *use changes and flood risk - SC060092/R1*. Bristol, UK.: Environment Agency. Retrieved from
590 https://www.gov.uk/government/uploads/system/uploads/attachment_data/file/480785/Land_use_change_and
591 _flood_risk_report.pdf
592 Ghaffari, G., Keesstra, S., Ghodousi, J., & Ahmadi, H. (2010). SWAT-simulated hydrological impact of land-use change in
593 the Zanjanrood Basin, Northwest Iran. *Hydrological Processes*, *24*, 892–903. doi:10.1002/hyp.7530
594 GREHYS, G. de recherche en hydrologie statistique. (1996). Presentation and review of some methods for regional flood
595 frequency analysis. *Journal of Hydrology*.
596 Gupta, S., Mohanty, B. P., & Köhne, M. (2006). Soil Hydraulic Conductivities and their Spatial and Temporal Variations in a
597 Vertisol. *Soil Science Society of America Journal*, *70*(6), 1872. doi:10.2136/sssaj2006.0201
598 Gupta, V. K., & Waymire, E. (1990). Multiscaling properties of spatial rainfall and river flow distributions. *Journal of*
599 *Geophysical Research*, *95*(D3), 1999. doi:10.1029/JD095iD03p01999
600 Hopmans, J. W., Nielsen, D. R., & Bristow, K. L. (2002). How useful are small-scale soil hydraulic property measurements
601 for large-scale vadose zone modeling? *Geophysical Monograph Series*, *129*, 247–258. doi:10.1029/129GM20
602 Hu, W., Shao, M., Wang, Q., Fan, J., & Horton, R. (2009). Temporal changes of soil hydraulic properties under different
603 land uses. *Geoderma*, *149*(3-4), 355–366. doi:10.1016/j.geoderma.2008.12.016
604 Hundecha, Y., & Bárdossy, A. (2004). Modeling of the effect of land use changes on the runoff generation of a river basin
605 through parameter regionalization of a watershed model. *Journal of Hydrology*, *292*, 281–295.
606 doi:10.1016/j.jhydrol.2004.01.002
607 Jung, I. W., Chang, H., & Moradkhani, H. (2011). Quantifying uncertainty in urban flooding analysis considering hydro-
608 climatic projection and urban development effects. *Hydrology and Earth System Sciences*, *15*(2), 617–633.
609 doi:10.5194/hess-15-617-2011
610 Kodesová, R., Jirku, V., Kodes, V., Muhlhanselová, M., Nikodem, A., & Žigová, A. (2011). Soil structure and soil hydraulic
611 properties of Haplic Luvisol used as arable land and grassland. *Soil and Tillage Research*, *111*(2), 154–161.
612 doi:10.1016/j.still.2010.09.007
613 Koinig, K., Shotyk, W., Lotter, A., & Ohlendorf, C. (2003). 9000 years of geochemical evolution of lithogenic major and trace
614 elements in the sediment of an …. *Journal of Paleolimnology*, *30*, 307–320. Retrieved from
615 http://www.springerlink.com/index/G548V1W32W731523.pdf\nfile:///Users/whobbs/Documents/PDFs/Papers2
616 /Koinig/2003/J Paleolimnol 2003 Koinig.pdf\npapers2://publication/uuid/0A0CA68B-51CB-426B-AEC4-
617 16055B490C9D
618 Kumar, S., Anderson, S. H., Bricknell, L. G., Udawatta, R. P., & Gantzer, C. J. (2008). Soil hydraulic properties influenced by
619 agroforestry and grass buffers for grazed pasture systems. *Journal of Soil and Water Conservation*, *63*(4), 224–232.
620 doi:10.2489/63.4.224
621 Kuraś, P. K., Alila, Y., & Weiler, M. (2012). Forest harvesting effects on the magnitude and frequency of peak flows can
622 increase with return period. *Water Resources Research*, *48*(1), 1–19. doi:10.1029/2011WR010705
623 Lovell, S. T., & Sullivan, W. C. (2006). Environmental benefits of conservation buffers in the United States: Evidence,
624 promise, and open questions. *Agriculture, Ecosystems and Environment*, *112*(4), 249–260.

doi:10.1016/j.agee.2005.08.002
Mao, D., & Cherkauer, K. a. (2009). Impacts of land-use change on hydrologic responses in the Great Lakes region. *Journal of Hydrology*, *374*, 71–82. doi:10.1016/j.jhydrol.2009.06.016
Marshall, M. R., Ballard, C. E., Frogbrook, Z. L., Solloway, I., Mcintyre, N., Reynolds, B., & Wheater, H. S. (2014). The impact of rural land management changes on soil hydraulic properties and runoff processes: Results from experimental plots in upland UK. *Hydrological Processes*, *28*(4), 2617–2629. doi:10.1002/hyp.9826
McCormick, B. C., Eshleman, K. N., Griffith, J. L., & Townsend, P. a. (2009). Detection of flooding responses at the river basin scale enhanced by land use change. *Water Resources Research*, *45*(8), 1–15. doi:10.1029/2008WR007594
Moriasi, D. N., Arnold, J. G., Van Liew, M. W., Binger, R. L., Harmel, R. D., & Veith, T. L. (2007). Model evaluation guidelines for systematic quantification of accuracy in watershed simulations. *Transactions of the ASABE*, *50*(3), 885–900. doi:10.13031/2013.23153
Morrison, J. E., & Smith, J. a. (2002). Stochastic modeling of flood peaks using the generalized extreme value distribution. *Water Resources Research*, *38*(12), 41–1–41–12. doi:10.1029/2001WR000502
Nie, W., Yuan, Y., Kepner, W., Nash, M. S., Jackson, M., & Erickson, C. (2011). Assessing impacts of Landuse and Landcover changes on hydrology for the upper San Pedro watershed. *Journal of Hydrology*, *407*(1-4), 105–114. doi:10.1016/j.jhydrol.2011.07.012
Niemeyer, R. J., Fremier, a. K., Heinse, R., Chávez, W., & DeClerck, F. a. J. (2014). Woody Vegetation Increases Saturated Hydraulic Conductivity in Dry Tropical Nicaragua. *Vadose Zone Journal*, *13*(1). doi:10.2136/vzj2013.01.0025
Öztürk, M., Copty, N. K., & Saysel, A. K. (2013). Modeling the impact of land use change on the hydrology of a rural watershed. *Journal of Hydrology*, *497*, 97–109. doi:10.1016/j.jhydrol.2013.05.022
Quilbé, R., Rousseau, a. N., Moquet, J.-S., Savary, S., Ricard, S., & Garbouj, M. S. (2008). Hydrological responses of a watershed to historical land use evolution and future land use scenarios under climate change conditions. *Hydrology and Earth System Sciences*, *12*, 101–110. doi:10.5194/hess-12-101-2008
Rivera, M. (2008). *Determinación de la dinámica del agua en el sistema agroforestal Quesungual e identificación de factores suelo-planta para el mejoramiento de la productividad del agua en los cultivos*. Universidad Nacional de Colombia. Retrieved from http://www.bdigital.unal.edu.co/706/
Robinson, J. S., & Sivanapalan, M. (1997). Temporal scales and hydrological regimes : Implications for flood frequency scaling interactions can help identify different hydrological Using the theoretical regimes are characterized by low values of the coefficient of variation , peaks , while fast re, *33*(12), 2981–2999.
Robinson, M., Cognard-Plancq, A. L., Cosandey, C., David, J., Durand, P., F??hrer, H. W., … Zollner, A. (2003). Studies of the impact of forests on peak flows and baseflows: A European perspective. *Forest Ecology and Management*, *186*(1-3), 85–97. doi:10.1016/S0378-1127(03)00238-X
Ruiz-Villanueva, V., Stoffel, M., Bussi, G., Francés, F., & Bréthaut, C. (2015). Climate change impacts on discharges of the Rhone River in Lyon by the end of the twenty-first century: model results and implications. *Regional Environmental Change*, *15*(3), 505–515. doi:10.1007/s10113-014-0707-8
Sajikumar, N., & Remya, R. S. (2014). Impact of land cover and land use change on runoff characteristics. *Journal of Environmental Management*, 1–9. doi:10.1016/j.jenvman.2014.12.041
Salazar, S., Francés, F., Komma, J., Blume, T., Francke, T., Bronstert, a., & Blöschl, G. (2012). A comparative analysis of the effectiveness of flood management measures based on the concept of "retaining water in the landscape" in different European hydro-climatic regions. *Natural Hazards and Earth System Science*, *12*(11), 3287–3306. doi:10.5194/nhess-12-3287-2012
Salemi, L. F., Groppo, J. D., Trevisan, R., de Moraes, J. M., de Barros Ferraz, S. F., Villani, J. P., … Martinelli, L. A. (2013). Land-use change in the Atlantic rainforest region: Consequences for the hydrology of small catchments. *Journal of Hydrology*, *499*, 100–109. doi:10.1016/j.jhydrol.2013.06.049
Saxton, K. E., & Rawls, W. J. (2006). Soil Water Characteristic Estimates by Texture and Organic Matter for Hydrologic Solutions. *Soil Science Society of America Journal*, *70*(5), 1569. doi:10.2136/sssaj2005.0117
Schwärzel, K., Carrick, S., Wahren, A., Feger, K.-H., Bodner, G., & Buchan, G. (2011). Soil Hydraulic Properties of Recently Tilled Soil under Cropping Rotation Compared with Two-Year Pasture. *Vadose Zone Journal*, *10*(1), 354. doi:10.2136/vzj2010.0035
Srinivas, V. V., Tripathi, S., Rao, a. R., & Govindaraju, R. S. (2008, January). Regional flood frequency analysis by combining self-organizing feature map and fuzzy clustering. *Journal of Hydrology*. doi:10.1016/j.jhydrol.2007.09.046
Stehr, a., Aguayo, M., Link, O., Parra, O., Romero, F., & Alcayaga, H. (2010). Modelling the hydrologic response of a mesoscale Andean watershed to changes in land use patterns for environmental planning. *Hydrology and Earth System Sciences*, *14*(10), 1963–1977. doi:10.5194/hess-14-1963-2010
Udawatta, R. P., Krstansky, J. J., Henderson, G. S., & Garrett, H. E. (2002). Agroforestry practices, runoff, and nutrient loss: a paired watershed comparison. *Journal of Environmental Quality*, *31*(4), 1214–1225. doi:10.2134/jeq2002.1214
Vaskôva, I. (2001). *Cálculo de las curvas IDF mediante la incorporación de las propiedades de escala y de dependencia temporales*. Universitat Politècnica de València.
Vélez, J. J., Puricelli, M., López Unzu, F., & Francés, F. (2009). Parameter extrapolation to ungauged basins with a

684 hydrological distributed model in a regional framework. *Hydrology and Earth System Sciences Discussions*, *13*, 229–
685 246. doi:10.5194/hessd-4-909-2007
686 Villarini, G. (2010). Analysis of the stationarity of flood peaks in the United States. In *Workshop on Nonstationarity,*
687 *Hydrologic Frequency Analysis, and Water Management* (pp. 81–97). Retrieved from www.cwi.colostate.edu
688 Whitfield, P. H. (2012). Floods in future climates: A review. *Journal of Flood Risk Management*, *5*(4), 336–365.
689 doi:10.1111/j.1753-318X.2012.01150.x
690 Wijesekara, G. N., Gupta, a., Valeo, C., Hasbani, J. G., Qiao, Y., Delaney, P., & Marceau, D. J. (2012). Assessing the impact
691 of future land-use changes on hydrological processes in the Elbow River watershed in southern Alberta, Canada.
692 *Journal of Hydrology*, *412-413*, 220–232. doi:10.1016/j.jhydrol.2011.04.018
693 Zhang, Y., Smith, J. a., & Baeck, M. L. (2001). The hydrology and hydrometeorology of extreme floods in the Great Plains
694 of Eastern Nebraska. *Advances in Water Resources*, *24*, 1037–1049. doi:10.1016/S0309-1708(01)00037-9
695 Zhou, X., Lin, H. S., & White, E. a. (2008). Surface soil hydraulic properties in four soil series under different land uses and
696 their temporal changes. *Catena*, *73*(2), 180–188. doi:10.1016/j.catena.2007.09.009
697 Zimmermann, B., Elsenbeer, H., & De Moraes, J. M. (2006). The influence of land-use changes on soil hydraulic properties:
698 Implications for runoff generation. *Forest Ecology and Management*, *222*(1-3), 29–38.
699 doi:10.1016/j.foreco.2005.10.070
700